AFRL-AFOSR-VA-TR-2023-0276

Insulator-Metal Transition and Superconductivity in CuCi

Kopelevitch, Lakov
Universidade Estadual de Campinas
Rua da Reitoria s/nº Cidade Universitária
CAMPINAS SP, , 13083-872
BR

02/17/2023
Final Technical Report

Air Force Research Laboratory
Air Force Office of Scientific Research
Arlington, Virginia 22203
Air Force Materiel Command

REPORT DOCUMENTATION PAGE

PLEASE DO NOT RETURN YOUR FORM TO THE ABOVE ORGANIZATION.

1. REPORT DATE	2. REPORT TYPE	3. DATES COVERED	
20230217	Final	START DATE 20170415	END DATE 20210414

4. TITLE AND SUBTITLE
Insulator-Metal Transition and Superconductivity in CuCi

5a. CONTRACT NUMBER	5b. GRANT NUMBER	5c. PROGRAM ELEMENT NUMBER
	FA9550-17-1-0132	61102F
5d. PROJECT NUMBER	**5e. TASK NUMBER**	**5f. WORK UNIT NUMBER**

6. AUTHOR(S)
Lakov Kopelevitch

7. PERFORMING ORGANIZATION NAME(S) AND ADDRESS(ES)
Universidade Estadual de Campinas
Rua da Reitoria s/nº Cidade Universitária
CAMPINAS SP 13083-872
BR

8. PERFORMING ORGANIZATION REPORT NUMBER

9. SPONSORING/MONITORING AGENCY NAME(S) AND ADDRESS(ES)	10. SPONSOR/MONITOR'S ACRONYM(S)	11. SPONSOR/MONITOR'S REPORT NUMBER(S)
Air Force Office of Scientific Research 875 N. Randolph St. Room 3112 Arlington, VA 22203	AFRL/AFOSR IOS	AFRL-AFOSR-VA-TR-2023-0276

12. DISTRIBUTION/AVAILABILITY STATEMENT
A Distribution Unlimited: PB Public Release

13. SUPPLEMENTARY NOTES

14. ABSTRACT
Our results obtained under AFOSR support provided an unambigous experimental evidence for the CuCl oxidation at ambient conditions resulting in the formation of antiferromagnetic clinoatacamite Cu2Cl(OH)3 and CuO phases, intimately related to the measured localized superconductivity. Superconducting effects observed for T < TN2 = 6.5 K in the case of Cu2Cl(OH)3 and in the temperature interval TN2 < T < 340 K in the case of CuO coincide with fluctuating short-ranged ordered magnetization measured in these materials, resembling the behavior of RVB quantum spin liquid proposed for cuprates. Thus, our results strengthen the Anderson´s conjecture on superconductivity in CuCl and may have far-reaching consequences.

15. SUBJECT TERMS

16. SECURITY CLASSIFICATION OF:			17. LIMITATION OF ABSTRACT	18. NUMBER OF PAGES
a. REPORT	b. ABSTRACT	c. THIS PAGE		
U	U	U	SAR	22

19a. NAME OF RESPONSIBLE PERSON	19b. PHONE NUMBER *(Include area code)*
STACY MANNI	0000 0000

Final Technical Report

Principal Investigator: Dr. Iakov Kopelevitch (Yakov Kopelevich)

Instituto de Física "Gleb Wataghin", Universidade Estadual de Campinas-UNICAMP. Adress: Rua Sergio Buarque de Holanda, 777, cidade Universitária Zeferino Vaz, Campinas-São Paulo-Brazil (zip code: 13083-859)

Grant/Contract Number: FA9550-17-1-0132

Grant/ContractTitle: *"Insulator-Metal Transition and Superconductivity in CuCl"*

Extended Abstract.

Before the cuprate era, experiments performed on Copper Chloride (CuCl) were a major hope related to high-temperature superconductivity (high-T_c) [C. W. Chu et al., Phys Rev. B 18, 2116 (1978)]. After discovery of high-T_c superconductivity in Copper Oxide (cuprates) compounds [J. G. Bednorz and K. A. Müller, Z. Phys. B 64, 189 (1986)], enormous both experimental and theoretical efforts have been dedicated to understand its origin. Now, several decades later, there is still no consensus regarding the microscopic mechanism of the cuprate superconductivity. One of the possible scenarios is the "resonating valence-bond" (RVB) theory [P. W. Anderson, Science 235, 1196 (1987)]. The RVB theory considers the superexchange antiferromagnetic interaction between Cu and O atoms in the copper-oxygen (Cu-O) planes as fundamental for the occurrence of high temperature superconductivity in cuprates. The preexisting spin singlet pairs of the insulating state become superconducting pairs when the insulator is doped with electrons or holes. The Anderson´s comment regarding CuCl [P. W. Anderson, Science 235, 1196 (1987)] is particularly intriguing in the context of our present work: "Finally, I would call attention to the numerous unreproducible reports of high temperature superconductivity in special samples of CuCl. In every case it is reasonable to imagine a surface layer of Cu^{2+} with or without the appropriate degree of oxidation; such reports should sharpen the search for still more "resonating valence-bond" (RVB) superconductors". Our results provided an unambigous experimental evidence for the CuCl oxidation at ambient conditions resulting in the formation of antiferromagnetic clinoatacamite $Cu_2Cl(OH)_3$ and CuO phases, intimately related to the measured localized superconductivity. Superconducting effects observed for $T < T_{N2} = 6.5$ K in $Cu_2Cl(OH)_3$ and in the temperature interval $T_{N2} < T < 340$ K in the case of CuO coincide with fluctuating short-ranged ordered magnetization measured in these materials, resembling the behavior of RVB quantum spin liquid proposed for cuprates.

I. Shedding light on the origin of metallic state in CuCl.

Several decades ago, the observed electrical breakdown in CuCl has been attributed to the formation of free Cu filaments of a few microns diameter [A. L. Gentile, Appl. Phys. Lett. 9, 237 (1966)]. However, our observation of the intermittent time dependence (bi- or multi-stability) of the insulating state [Y. Kopelevich et al., Physica C 514, 237 (2015)] cannot be easily understood assuming the formation of Cu "wires". One can also argue against a Zener model for dielectric breakdown. Indeed, taking the gap energy in CuCl, E_g = 3.4 eV and a lattice constant a = 5.41Å, one estimates the threshold field for dielectric breakdown E_{th} ~ 70 MV/cm which is much higher than the applied in the experiments electric field E ~ 450 V/cm. Besides, our results strongly suggest that the metallic-type conductivity in CuCl is governed by the intergrain boundaries.

In what follows, we report the results that provide us with a new insight on the origin of the electric (E)-field driven metallic state in CuCl.

The samples were prepared pressing the commercially available (Sigma Aldrich and Alfa Aesar) CuCl powder into cylindrical pellets of ~ 5 mm diameter (D) with the thickness ranging from 0.1 to 1 mm. The pressure, typically ~ 1 GPa, was applied using a hydraulic press and a steel pastillator. During the measurements, the samples were kept in an inert atmosphere of He gas inside of commercial cryostats from Janis or PPMS (Quantum Design). The equipment allows the variation of the temperature (T) and magnetic field (B) in the intervals: 2 K < T < 350 K and - 9 T < B < 9 T. Magnetization measurements were performed by menas of SQUID magnetometer from Quantum Design.

The electric transport measurements were made using silver paste (Ag) electrodes placed on upper and lower faces of the sample, as shown in Fig. 1. Current-voltage (I-V) characteristics and the resistance vs. time R(t) measurements were performed in the voltage-generator mode. The resistance temperature and magnetic field dependencies R(T,B) were recorded at constant applied current, Fig. 1.

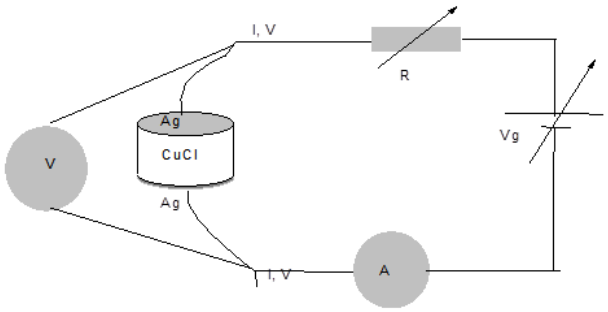

Fig. 1. Electric transport measurements setup.

Here, we present and analyze the results obtained for a few out of tens studied samples.

Figures 2 and 3 demonstrate the electric-field-driven transitions between high (low)- and low (high) -resistance states mesured in CuCl at T = 300 K, and its intermittent time dependence varying the applied voltage (V_g) amplitude or polarity.

Noting, the initially applied electric field can either trigger the insulator-metal (I-M) transition (Fig. 2) or drive the sample from its metallic state back to the insulating one (Fig. 3). We note also that in the samples that possess larger size particles, i. e. the samples having a smaller surface area, practically no electric-field effect was observed, indicating that the electrical transport is governed by the intergrain surfaces/boundaries.

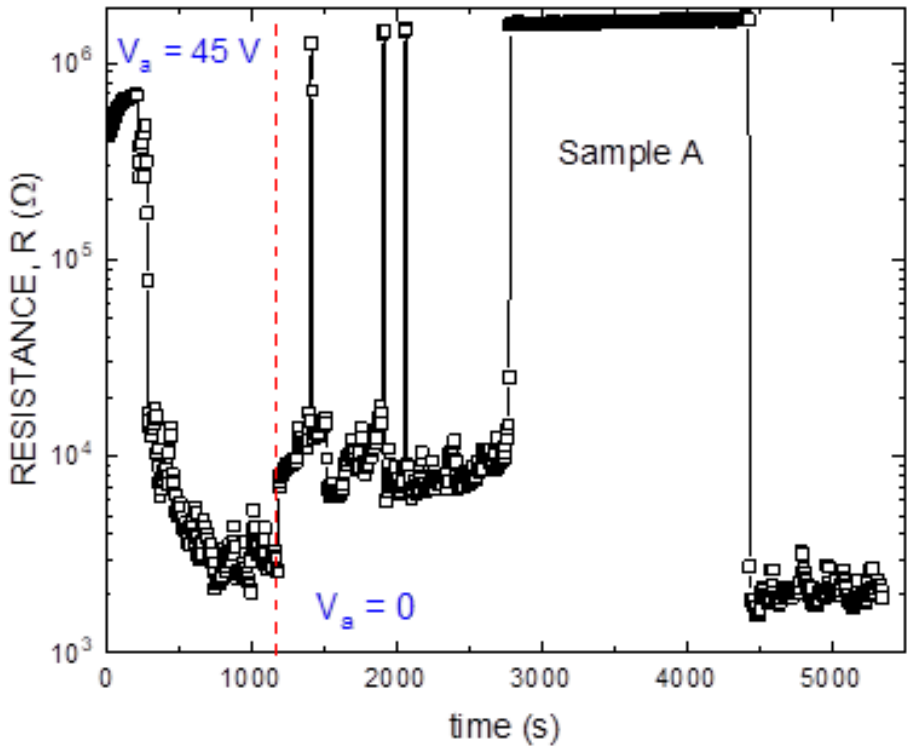

Fig. 2. Electric-field-driven transition and its intermittent time dependence between high- and low-resistance states measured in our CuCl sampe (A).

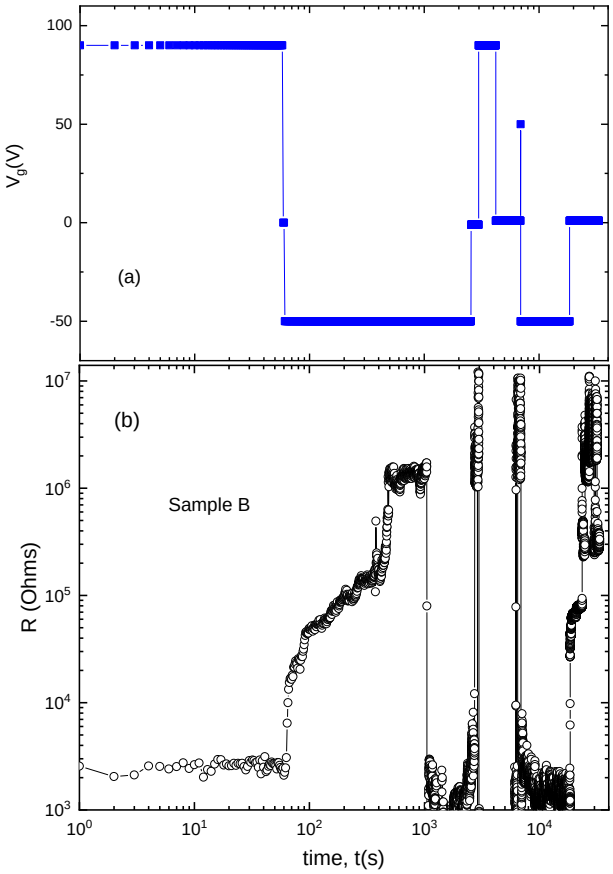

Fig. 3. Electric-field-driven transition between low- and high - resistance states in CuCl sample B, and its intermittent time dependence (b), in response to the variation of applied voltage (a).

Aiming to clarify the origin of metastable conducting state in CuCl, we have studied temperature dependencies of the resistance R(T) as well as current-voltage I-V characteristics (IVC) at various temperatures.

Figure 4 presents R(T) measured in Ohmic regime for the sample A. As can be seen from Fig. 4, $R(T) \sim T^{3/2}$, demonstrating metallic ($dR/dT > 0$) behavior in a broad temperature range. For $T < T_{min} \sim 20$ K, $dR/dT < 0$, providing evidence for the electron localization effects or/and enhancement of the electron scattering rate.

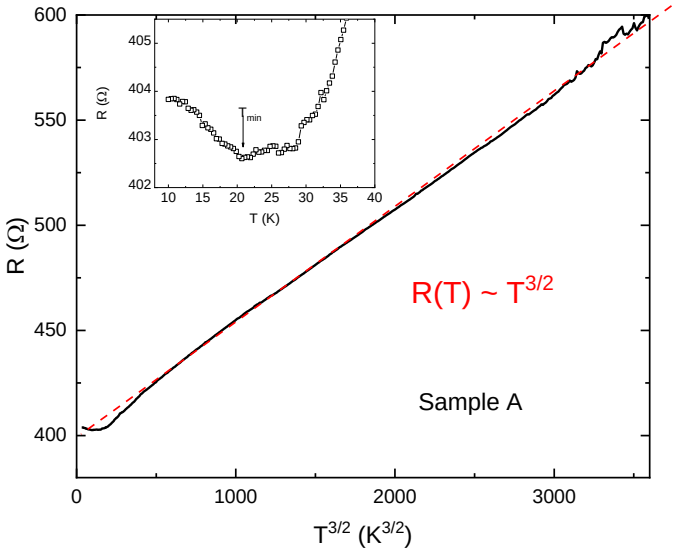

Fig. 4. Temperature dependence of the resistance R(T) measured for CuCl sample A in the metallic state. The broken red line corresponds to the power law $R(T) \sim T^{3/2}$. Inset shows the low-temperature portion of R(T) demonstrating minimum at $T_{min} \approx 20$ K.

The resistance behavior, similar to that ptresented in Fig.4 has been obtained for all CuCl samples in the low-resistance state. The metallic behvaior of the resistance $R(T) \sim T^{1.2}$ measured for another CuCl sample after application of electric field, as well as the insulator-like state at temperature below $T_{min} \sim 23$ K can be clearly seen in Fig. 5.

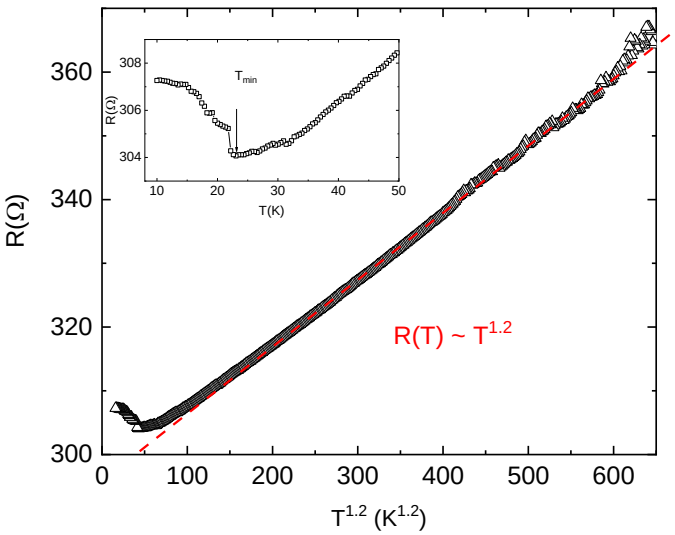

Fig. 5. Temperature dependence of the resistance R(T) measured for another CuCl sample in the metallic state (see also Fig. 4). The broken red line corresponds to the power law $R(T) \sim T^{1.2}$. Inset shows the low-temperature portion of R(T) demonstrating minimum at $T_{min} \approx 23$ K.

The resistance behavior shown in Fig. 4 and Fig. 5 agrees with that predicted for one-dimensional (1D) electronic quantum fluids [T. Giamarchi and H. J. Schulz, Phys. Rev. B 37, 325 (1988)]. In agreement with our observations, the theory by Giamarchi and Schulz (GS), that considers both quenched disorder and electron-electron interactions, predicts $R(T) \sim T^{1+\gamma}$ where $\gamma \geq 0$ depends on the disorder. According to GS, at high enough temperatures, the resistivity decreases with temperature decrease ($dR/dT > 0$) , and below $T = T_{loc}$ the resistance starts to increase ($dR/dT < 0$). This allows us to identify T_{loc} with T_{min} (see Figs. 4 and 5). Furthermore, according to GS, the delocalized phase ($T > T_{min}$) is dominated by superconducting fluctuations, whereas the localized phase ($T < T_{min}$) corresponds to a charge - density wave (CDW) pinned by a quenched disorder (crystallographical defects or/and impurities).

Corroborating these ideas, we have observed non-linear current-voltage (I-V) characteristics for $T < T_{min}$ (Fig. 6a) and ohmic I-V characteristics for $T > T_{min}$ [Fig. 6(b)]. As Fig. 6(a) illustrates, $I \sim V^{\alpha}$ with $\alpha = 1.5 \pm 0.1$, the behavior expected for sliding (above the depinning transition) CDW in one (1D) or two (2D) dimensions [C. R. Myers et al., PRB 47, 11171 (1993)].

At the same time, the observed R(T) in the metallic state of CuCl (Fig. 4 and Fig. 5) are also consistent with the electronic transport in magnetic and nearly magnetic metals in a vicinity of the quantum phase transition (QPT) [R. Ramazashvili, PRB 60, 7314 (1999); B.Andraka and A. M. Tsvelik, PRL 67, 2886 (1991)].

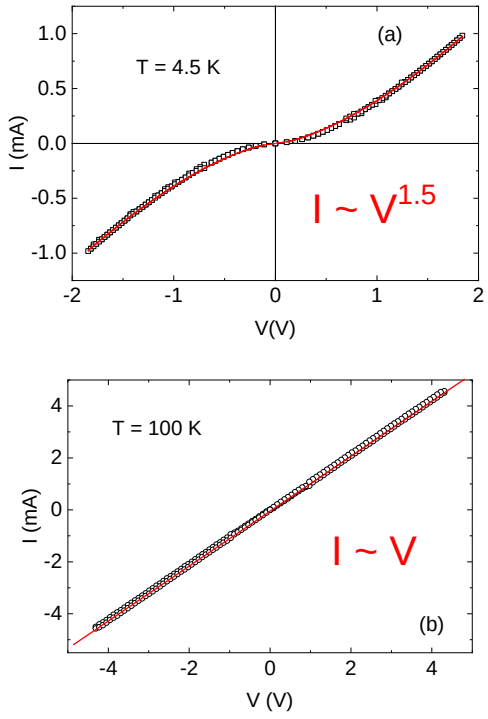

Fig. 6. Current-voltage (I-V) characteristics mesured for CuCl (sample A) in the electric-field-induced metallic state for $T < T_{min} = 20$ K (a) and $T > T_{min}$ (b) , see also Fig. 4.

For T > T_{min}, I-V characteristics demonstrate a complex behavior related to the switching between metallic and insulating states. As Fig. 7 demonstrates, the switching takes place after a certain number of I-V measuring cycles at a constant temperature.

In other words, our results provide a clear experimental evidence that the electric-field-driven metallic state in CuCl is out of equilibrium.

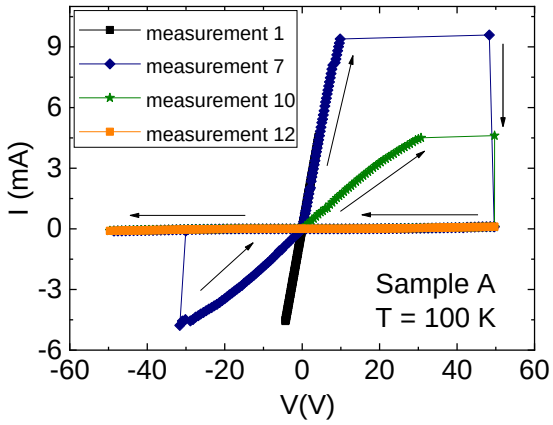

Fig. 7. Multiple I-V cycles measured for the CuCl sample A at T = 100 K demonstrating the transformation from metallic (curve 1) to insulating (curve 12) state.

Figures 8 and 9 illustrate in more details the transformation of Ohmic I-V characteristics [see also Fig. 6(b)] to strongly nonlinear I-V curves.

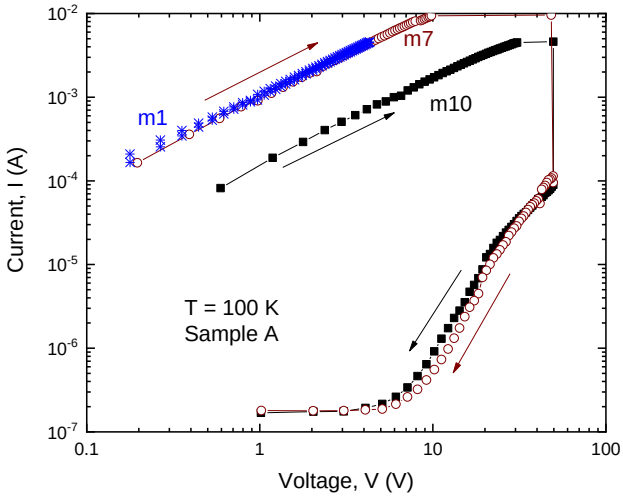

Fig. 8. Transformation of Ohmic I-V characteristics (metallic state) to strongly non-linear onces (insulator state) after several measuring cycles in CuCl.

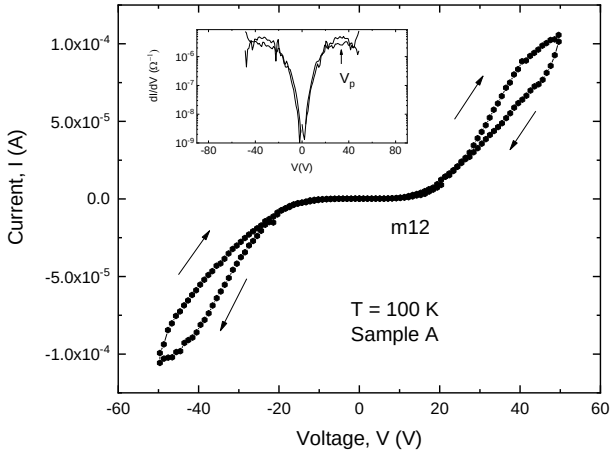

Fig. 9. I-V characteristic measured in CuCl after the voltage-cycling-induced metal-insilator transformation. Inset shows the differencional conductance G(V) = dI/dV with the maxima occurring at $|V_P| \approx 33$ V.

Noting, the I-V characteristic (12th measurement cycle), shown in Fig. 9 resembles that known for driven macroscopic elastic objects interacting with a quenched disorder [C. Reichhardt et al., Rep. Prog. Phys. 80 026501 (2017)], such as e. g. Abrikosov vortex lattices or CDW, where an interplay between inter-particle (e.g. vortices, Cooper pairs, or other electron states) and particle-quenched disorder interactions plays a crucial role. In these systems, an effective strength of the interactions can be controlled by the applied driving force. At low drives the particle motion is dominated by the quenched disorder (pinning) effects, leading to the plastic (channel-like) motion of some regions of the elastic medium with respect to other temporarily pinned regions. With increasing the driving force, (re)ordering or dynamic crystallization of the elastic medium takes place. According to theoretical models [[C. Reichhardt et al., Rep. Prog. Phys. 80 026501 (2017)], the peak in the differential conductance G(V) = dI/dV at $|V| = |V_p| \sim$ 33 V, see the inset in Fig. 9, is expected when the disordered electronic matter becomes dynamically more ordered for $V > V_p$, forming sliding electronic phases.The clock-wise hysteresis in I-V occurring for big enough applied voltage (Fig.9) suggests the 1D incommensurate particle flow.

Assuming that the delocalized phase ($T > T_{min}$) is dominated by superconducting fluctuations, it is tempting to relate the insulating state to pinned bosonic CDW (see below).

I.1. A role of CuO in the observed phenomena.

One of our findings is a striking similarity between magnetic and transport anomalies in CuO and CuCl, which we attribute to the traces of CuO in oxidized CuCl (see Fig. 10).

In the case of CuCl, the transient high-temperature superconductivity for temperature T < 230 K has been reported by C. W. Chu et al. [PRB 18, 2116 (1978)]. At the same time, CuO undergoes antiferromagnetic (AFM) transition at this temperature (T_{N2} = 230 K), as

well as the second transition at T_{N1} = 213 K [see, e. g., B. X. Yang et al., PRB 39, 4343 (1989) and refs. therein].

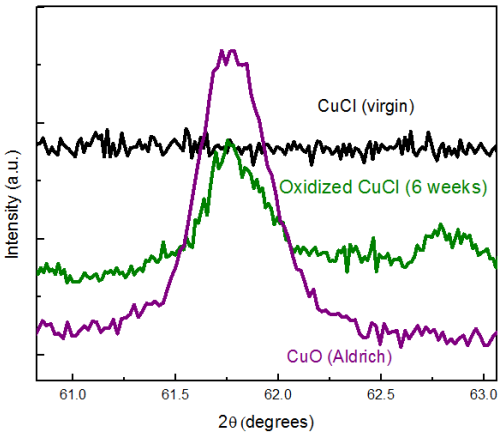

Fig. 10. X-ray Θ-2Θ diffraction patterns measured for virgin CuCl (Alfa Aesar) powder, CuO and the CuCl powder exposed to the ambient atmosphere for 6 weeks.

Here we present a new experimental evidence that the antiferromagnetic CuO stabilizes the metallic phase in CuCl. Furthermore, we show that polycrystalline CuO possesses anomalous metallicity for T > T_{N2} being consistent with either CDW or Cooper pair transport.

As Figure 11 illustrates, the resistance R(T) curves measured in the metallic state (Figs. 4 and 5) for two CuCl samples become unstable for temperatures just above the T_{N2} = 230 K corresponding to the AFM transition temperature in CuO.

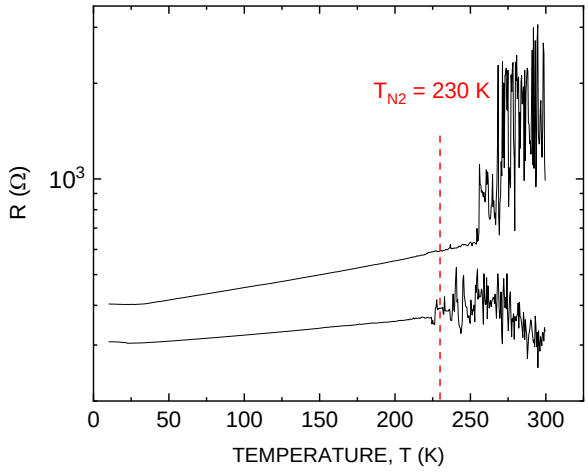

Fig. 11. R(T) measured in the metallic state of two CuCl samples (Fig. 4 and Fig. 5) is metastable for T > 230 K, corresponding to the Neel temperature T_{N2} = 230 K in CuO.

In the case of CuCl, the formation of Cu-CuCl metal-insulator interfaces responsible for the transient high-temperature superconductivity for temperature T < 230 K has been proposed by C. W. Chu et al. [PRB 18, 2116 (1978)].

Our data, however, strongly suggest the importance of CuO formation and its antiferromagnetic properties in the puzzling behavior of CuCl. For instance, the electronic reconstruction at the CuCl/CuO interfaces, expected for interfaces between Mott and band insulators [S. Okamoto and A, J. Millis, Nature 428, 630 (2004)] might be behind of the observed metallicity, CDW- and superconding-like behavior of CuCl.

However, studies of magnetrotransport properties of CuO are necessary before drawing any conclusion. Below, we present our experimental results that revealed previously unknown correlations between the electronic transport and antiferromagnetic ordering in CuO.

I.2. Effect of the antiferromagnetic ordering on electrical transport in CuO.

We have studied tens of well characterized (by means of XRD, SEM, EDS, and XPS techniques) CuO powdered samples [Copper (II) oxide powder, 99.99% (Aldrich)] with the average particle size of ~ 10 - 30 μm and flakes of polycrystalline CuO of the size ~ 5 x 3 x 0.5 mm^3. Selected scanning electron microscope (SEM) images of these samples are shown in Figures 12 - 15.

Fig. 12 presents SEM micrographs obtained for CuO powders demonstrating formation of wheel- and ball-like objects consisting of 10^5 - 10^6 CuO crystals of a micro- and sub-micrometer size. Fig. 13 gives a typical size of ~ 1 x 0.3 x 0.1 μm^3 for CuO single crystals. Fig. 14 shows that in some cases CuO meso-crystals are self-assembled in a form of flower-like objects.

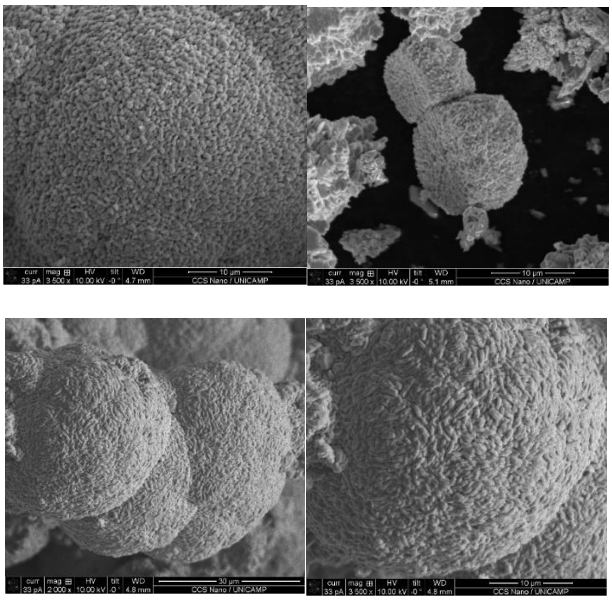

Fig. 12. Scanning electron microscope (SEM) micrograph of CuO powder demonstrating self-assembling.

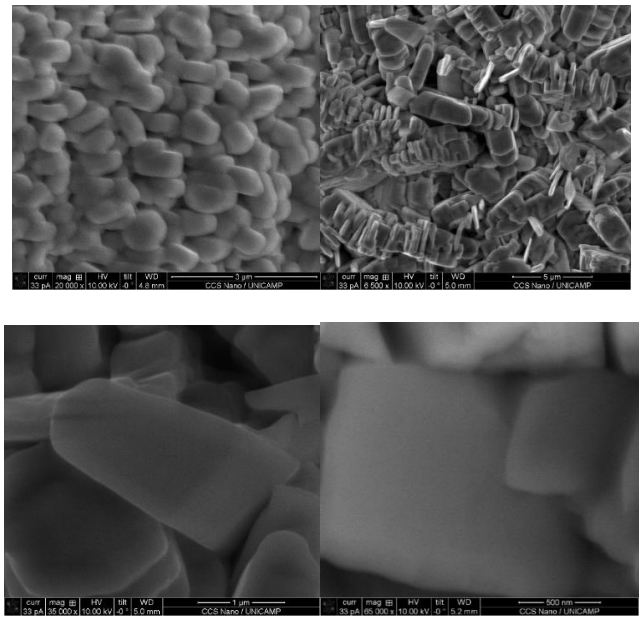

Fig. 13. SEM micrographs of CuO powder on a mesoscopic scale. Platelet-like CuO crystals with a characteristic size ~ 1 x 0.3 x 0.1 μm^3 can be clearly visualized.

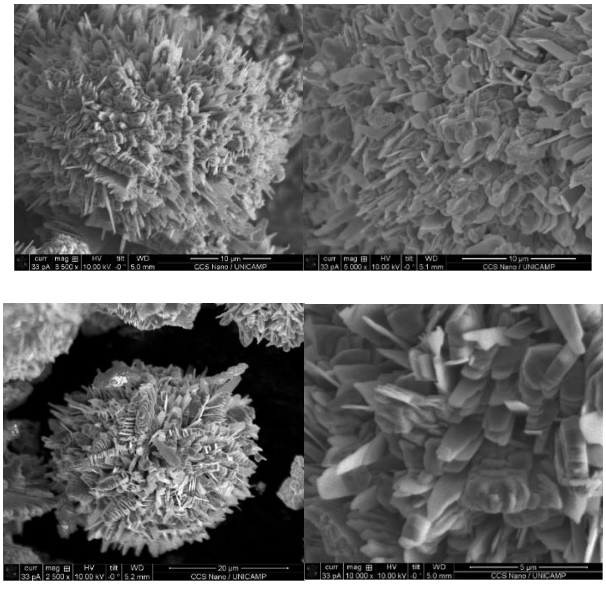

Fig. 14. SEM images of self-assembled CuO mesoscopic crystals in the flower-like shape.

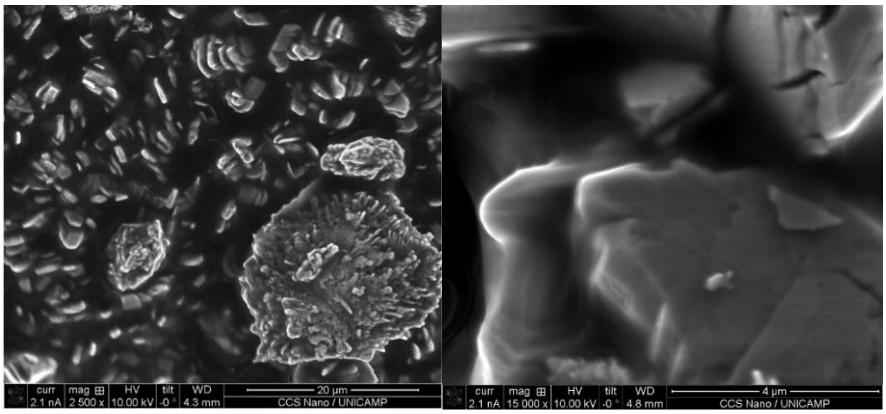

Fig. 15. SEM micrographs for polycrystalline CuO flakes consisting of dense-packed platelett-like mesoscopic crystals and flower-like islands.

Figure 15 presents SEM images of one of the measured CuO flakes. As can be seen from Fig. 15, CuO flakes are consist of dense-packed platelett-like CuO crystals and flower-like islands.

In what follows we present our key results obtained on the CuO flakes.

Results of magnetization measurements M (B, T), exemplified in Fig. 16, provide us with a clear expetrimental evidence for the antiferromagnetic transition at T_{N2} = 230 K, characteristic of CuO. Noting also the "anomalous" decrease of the magnetization on cooling for $T > T_{N2}$, resembling the normal state behavior of magnetization in underdoped cuprates, attributed to the response of antiferromagnetically coupled local Cu moments [T. Nakano et al., Phys. Rev. B 49, 16000 (1994); M. Hücker et al., Phys. Rev. B 78, 214507 (2008)].

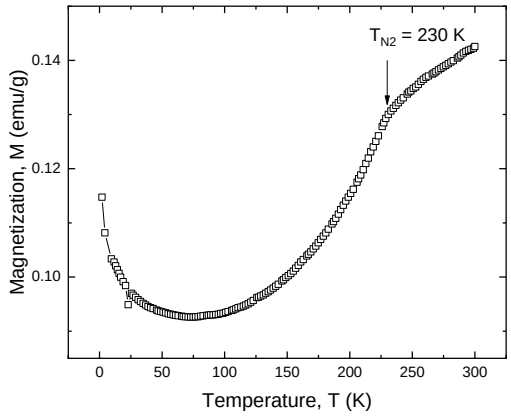

Fig. 16. Equilibrium magnetization M(T) measured for CuO flake at B = 5 T. M(T) demonstrates characteristic for the antiferromagnetic transition anomaly at the Neel temperature T_{N2} = 230 K.

Figures 17-20 present results of four-probe I-V characteristics measurements performed on CuO flake for temperatures below and above the Neel temperature $T_{N1} \approx$ 213 K.

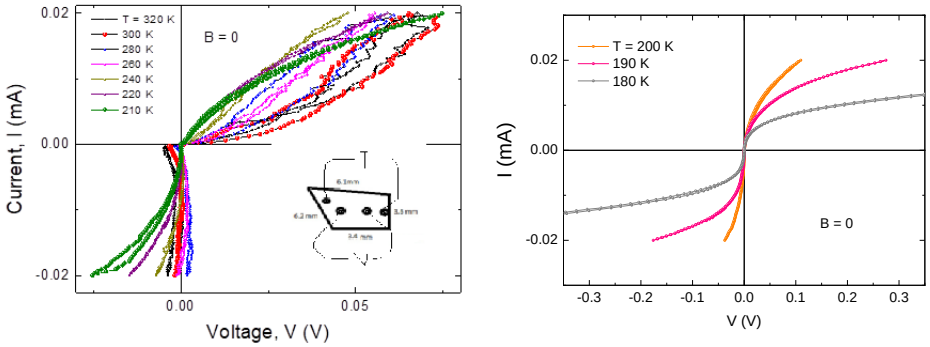

Fig. 17. I-V characteristics obtained for CuO flake for T > T_{N1} (left) and T< T_{N1} (right) at zero applied magnetic field (B = 0). Inset shows a schematic configuration of four Ag-paste electrodes.

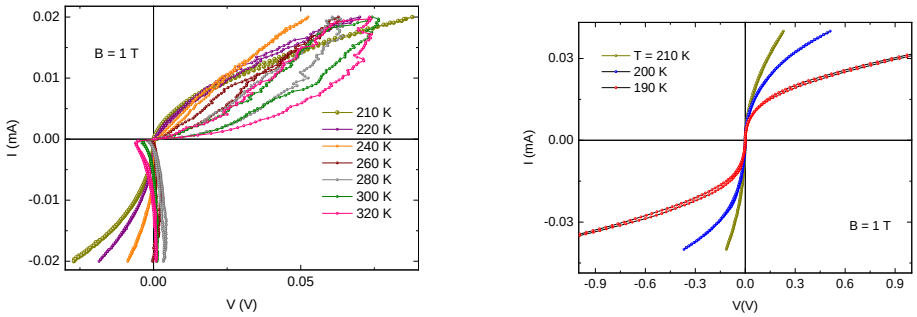

Fig. 18. I-V characteristics measutred for CuO flake for T > T_{N1} (left) and T< T_{N1} (right) at applied magnetic field B = 1 T.

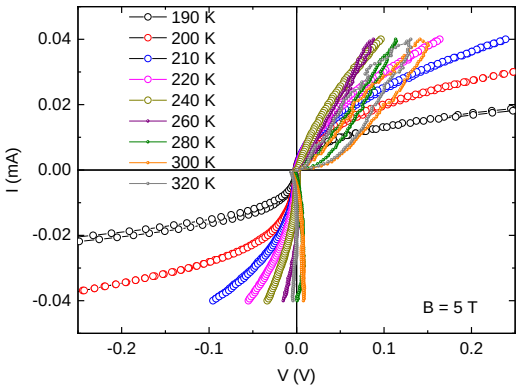

Fig. 19. I-V characteristics measutred for CuO flake in the temperature interval 190 K ≤ T ≤ 320 K and applied magnetic field B = 5 T.

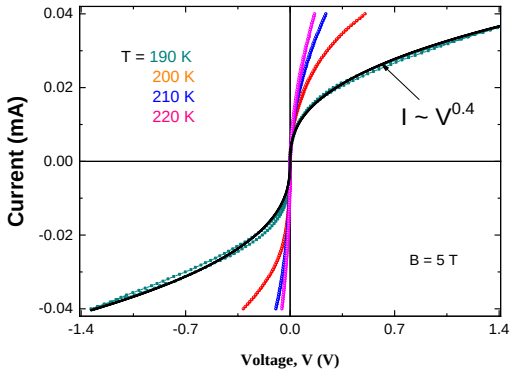

Fig. 20. I-V characteristics measured for CuO at B = 5 T at T < T_{N1}. Solid black line is power-law fitting of I ~ V^n (n = 0.4) measured at T = 190 K (< T_{N1}).

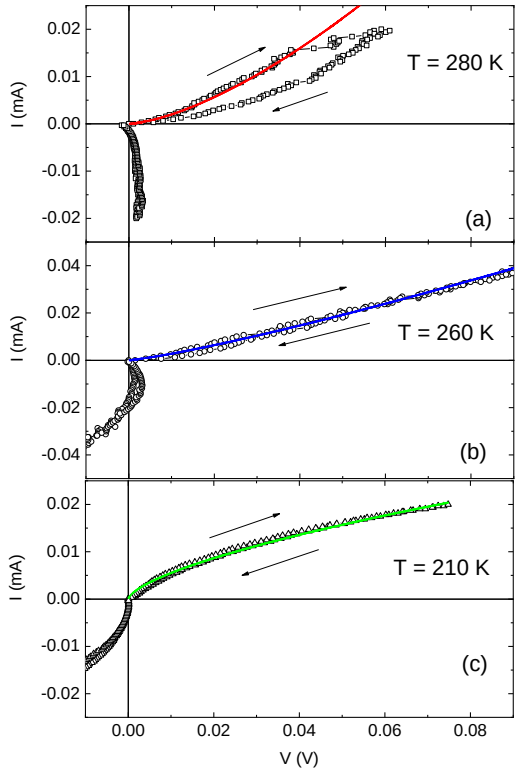

Fig. 21. Current-voltage (I-V) characteristics obtained for CuO flake in the low current/voltage limit at temperatures T > T_{N2} = 230 K (a, b) and the temperature just below T_{N1} =213 K (c). Solid lines correspond to the power law I ~ V^n with the exponent = 1.5 (a), n = 1.2 (b), and n = 0.65 (c).

Fugure 21 demonstrates a qualitative chnge in low-current/low-voltage I-V characteristics with temperature in a vicinity of the antiferromagnetic transition temperatures (T_{N1} and T_{N2}), providing eveidence for the coupling between electronic transport and antiferromagnetic ordering in CuO.

In order to further verify the existence of such interrelation, we measured temperature dependencies of the resitance R(T,I,B) at varios applied currents and magnetic fields. The R(T) obtained for I = 10 μA and magnetic fields B = 0 and B = 9 T are presented in Fig. 22.

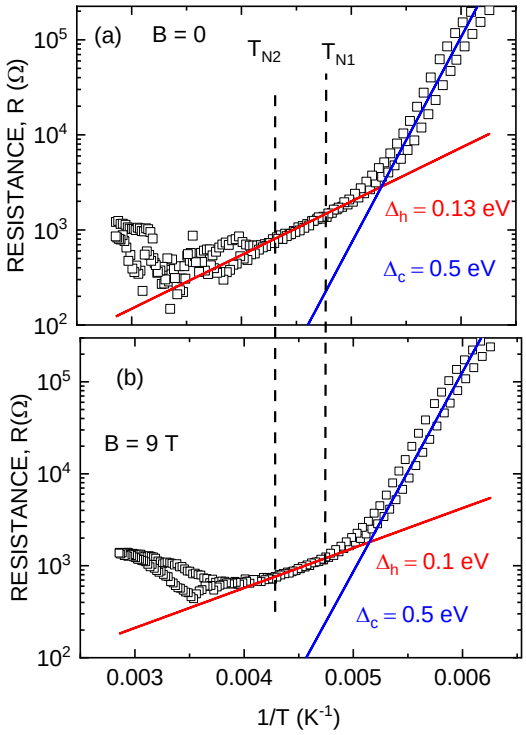

Fig. 22. R vs. 1/T measured in CuO flake for zero (a) and B = 9 T (b) applied magnetic field and measuring current I = 10 μA. Solid lines correspond to the exponential resistance behavior R(T) ~ exp(Δ/k_BT) with the activation energies $\Delta_c > \Delta_h$(B) (see text).

Figures 23 and 24 demonstrate the effect of measuring current on the resistance R(T,I,B) obtained in applied magnetic field B = 2 T.

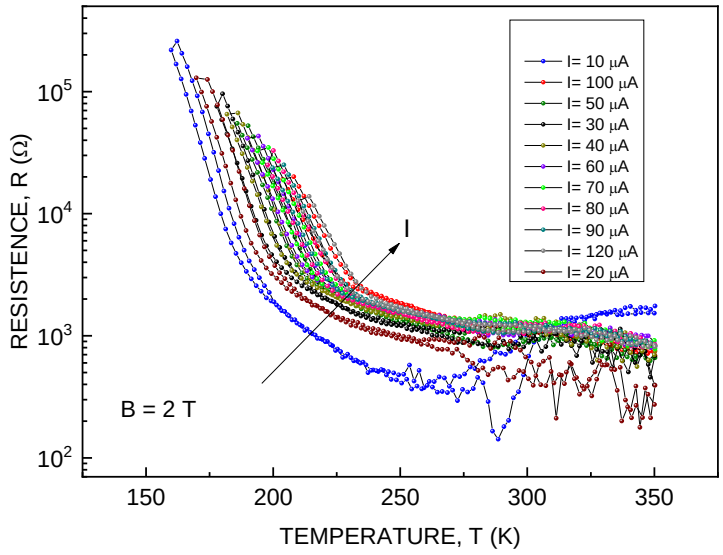

Fig. 23. RvsT measured in CuO flake for various applied currents and magnetic field B = 2 T.

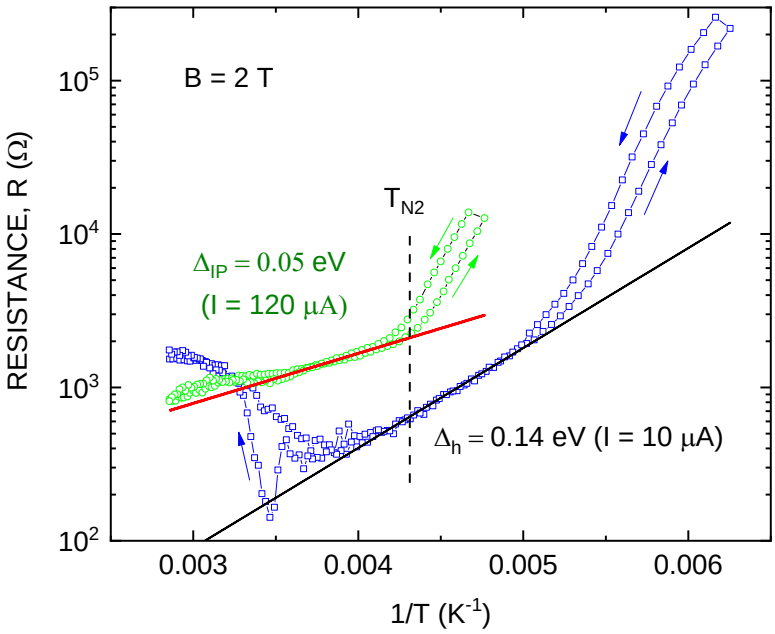

Fig. 24. The data of Fig. 23 plotted as R vs. 1/T for lowest (I = 10 μA) and highest (I = 120 μA) measuring currents. Noting a factor ~ 3 reduction of the activation energy, suppression of the resistance fluctuations, and R (T) ~ exp(Δ_{IP}/T) resistance behavior well above T_{N2} for I = 120 μA.

Figures 23 and 24 demonstrate the effect of measuring current on the resistance R(T,I,B) obtained in applied magnetic field B = 2 T.

The results presented in Figs. 16-24 provide us with the following experimental facts:

(1) The occurrence of non-linear, hysteretic, asymmetric and jumpy-like I-V characteristics (IVC) in the low current/voltage limit and $T > T_{N1}$.

(2) For $T > T_{N1}$ the absolute negative resistance (ANR) becomes evident and it increases in amplitude with the temperature increasing.

(3) The effects described in (1) and (2) vanish with lowering temperature ($T < T_{N1} \sim 213$ K) or increasing the applied voltage/current.

(4) In the low-temperature limit and large enough voltage (current), power-law $I \sim V^n$ characteristics were measured with the exponent $n = 0.5 \pm 0.1$ [Fig. 20 and Fig. 21(c)].

(5) In agreement with the IVC measurements, the temperature dependencies of the resistance R (T, I, B) revealed:

(5a) Hysteretic and jumpy-like R(T) in the low-current limit and $T > T_{N2} = 230$ K, as well as the transition from the insulator - ($dR/dT < 0$) to metallic- type ($dR/dT > 0$) behavior at $T \geq T_{N2}$ [Fig. 22(a) and Fig. 24]

(5b) For $T < T_{N2}$, $R(T) \sim \exp(\Delta/k_BT)$ with two different activation energies Δ_h ($T_{N1} < T < T_{N2}$) << Δ_c ($T < T_{N1}$), see Fig. 22.

(5c) Whereas, effect of the applied magnetic field is weak, it reduces both the activation gap $\Delta_h(B)$ and high-temperature resistance fluctuations, see Fig. 22.

(5d) High enough measuring current illiminates the anomalous "metallic" state leading for $T > T_{N2}$ to the insulating-type $R(T) \sim \exp(\Delta_{IP}/k_BT)$ with $\Delta_{IP} << \Delta_c$, Fig. 24.

Based on these experimental findings, we conclude that:

- the electronic transport in polycrystalline CuO is governed by both the antiferromagnetic spin ordering and applied current/voltage.

- the thermally activated resistance $R(T) \sim \exp(\Delta/k_BT)$ with the gap $\Delta(I, B)$ much smaller than the electron band energy gap ~ 2 eV [see e. g., A. Filippetti et al., PRL 95, 086405 (2005)] implies a collective electronic transport instead.

- $I \sim V^n$ ($n = 0.5 \pm 0.1$) agree with that expected for sliding (above the depinning transition) CDW in one (1D) or two (2D) dimensions [C. R. Myers et al., PRB 47, 11171 (1993)]. Hysteretic IVC and R(T) in the low-drive limit are consistent with the behavior of pinned CDW and/or other charge ordered objects.

- hysteretic and metastable IVC and R (T) in the low-drive limit are consistent with the behavior of pinned CDW [see e. g. G. Heinz et al., Synth. Metals 104, 61 (1999)], or other charge ordered objects such as stripes [J. Zaanen et al., Phys. Rev. B 40, 7391 (1989)]. Such a scenario is very appealing as various theoretical models consider the importance of the one-dimensional (1D) spin-charge density modulation (charge stripes) in the occurrence of high-temperature superconductivity [S. A. Kivelson et al., Nature 393, 550

(1998)]. Moreover, the quasi-1D charge stripes were vizualized in CuO single crystals [X. G. Zheng et al. Phys. Rev. Lett. 85, 5170 (2000)].

- Steps in IVC, IVC assymmetry, ANR and R(T, I) metastability are most pronounced in fluctuating short-ranged AFM state at $T > T_{N2}$, where the superconducting correlations are expected. Both superconducting-diode-like [A. M. Kadin, J. Appl. Phys. 68, 5741 (1990)] IVC, Fig. 21(a), and superconductivity-related fluctuations in IVC [Z. M. Wang et al., Appl. Phys. Lett. 114, 242601 (2019)] corraborate the superconducting scenario.

- Concerning the origin of possible high-temperature superconducting correlations in CuO, our special interest is due to current- and magnetic field - dependent characteristic energy $\Delta(I, B)$ in the temperature interval $T_{N1} < T < T_{N2}$ (Fig. 22), where the noncollinear incommensurate magnetic state coexists with the ferroelectric (FE) ordering [T. Kimura et. al., Nature Mat. 7, 291 (2008)].

Figure 25 illustrates the striking similarity of the data obtained on CuCl [C. W. Chu et al., Phys Rev. B 18, 2116 (1978)] and CuO (the present work). One can see that both compounds show anomalous drop of magnetic suseptibility (magnetization) and a sharp increase of electrical conductivity with temperature decreasing for T > 230 K, suggesting a common origin of the high-temperature anomalies in CuO and oxidized CuCl. In both compounds the insulating state sets in for T < 230 K which coincides with the antiferromagnetic transition temperature $T_{N2} \approx 230$ K for CuO.

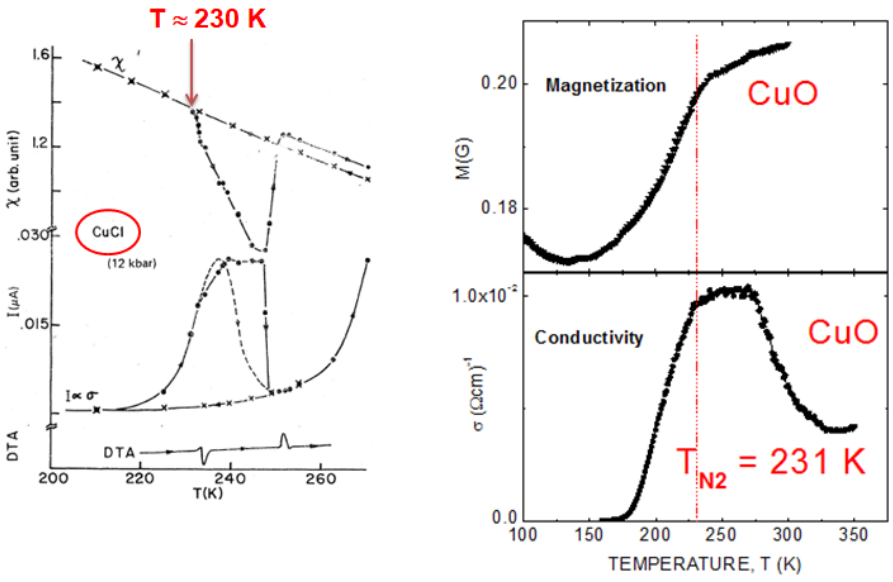

Fig. 25. Magnetic susceptibility (magnetization) and electrical conductivity measured for CuCl [C. W. Chu et al., Phys Rev. B 18, 2116 (1978).] (left panel) and CuO (this work) (right panel).

In the light of our finding of the localized superconductivity at Cu-$Cu_2(OH)_3Cl$ interfaces, we have studied the possibility of high-temperature superconductivity

associated with the CuO-Cu interfaces as well as with CuO itself. The results of our research in this direction are presented below.

II. Localized superconductivity in oxidized CuCl due to antiferromagnetic $Cu_2Cl(OH)_3$ phase.

Finally, we report our finding of localized superconductivity in the metallic state of CuCl originating from antiferromagnetic $Cu_2Cl(OH)_3$ phase in oxidized CuCl.

Figure 26 presents X-ray Θ-2Θ diffraction (XRD) patterns measured for virgin CuCl (Alfa Aesar) powder and the powder exposed to the ambient atmosphere for the time varying between 24 hours and 6 weeks. The development of the main peak of the clinotacamite $Cu_2Cl(OH)_3$ (copper oxychloride) arising due to the CuCl oxidation is clear.

In agreement with XRD data (Fig. 26), the magnetic moment m(T,H) measurements performed on oxidized for two weeks CuCl, revealed two antiferromagnetic transitions (see Fig.27): at $T_{N1} \approx 18$ K and $T_{N2} \approx 6.4$ K characteristic of $Cu_2Cl(OH)_3$ [X. G. Zheng et al. Phys. Rev. Lett. 95, 057201 (2005)].

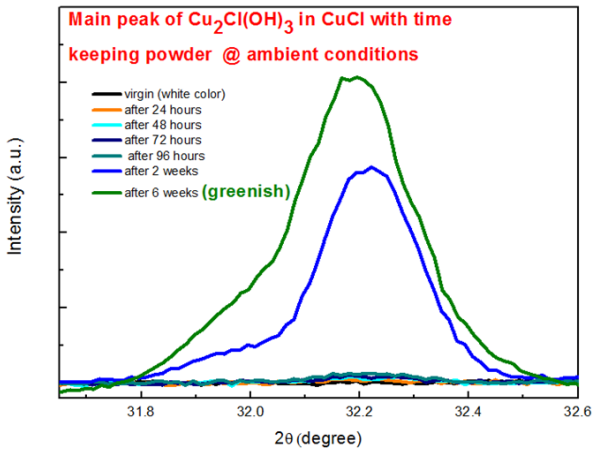

Fig. 26. X-ray Θ-2Θ diffraction (XRD) patterns measured for virgin CuCl (Alfa Aesar) powder and the powder exposed to the ambient atmosphere for the time varying between 24 hours and 6 weeks.

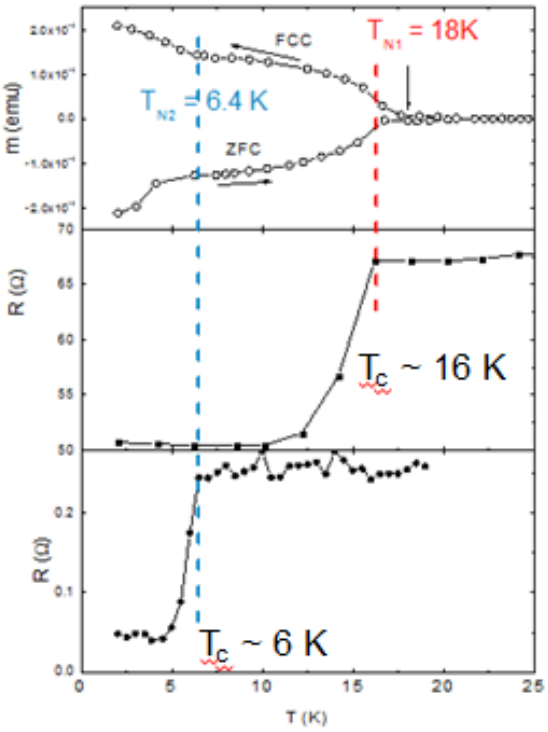

Fig. 27. Magnetic moment m(T) (top) and resistance R(T) (middle and bottom) measurements performed on oxidized (two weeks) CuCl; m(T) measurements were perfomed in applied field H = 10 Oe using SQUID magnetometer (Quantum Design) in the zero-field-cooled (ZFC) and field-cooled (FC) regimes. The results demonstrate a correlation between resistive and antiferromagnetic transitions at T_{N1} ~ 18 K and T_{N2} ~ 6.4 K characteristic to $Cu_2Cl(OH)_3$.

Figure 27 provides also the experimental evidence for the correlation between magnetic and resistive transitions recorded at zero applied magnetic field; the resistive transition temperature (T_c) coincides either with higher (T_{N1}) or lower (T_{N2}) Neel temperatures.

The measurements performed in applied magnetic field (Fig. 28 and Fig. 29) provide us with the unambiguous evidence for the superconducting origin of the resistively measured transitions. The obtained results strongly suggest that the superconductivity is localized at $CuCl/Cu_2(OH)_3Cl$ interfaces.

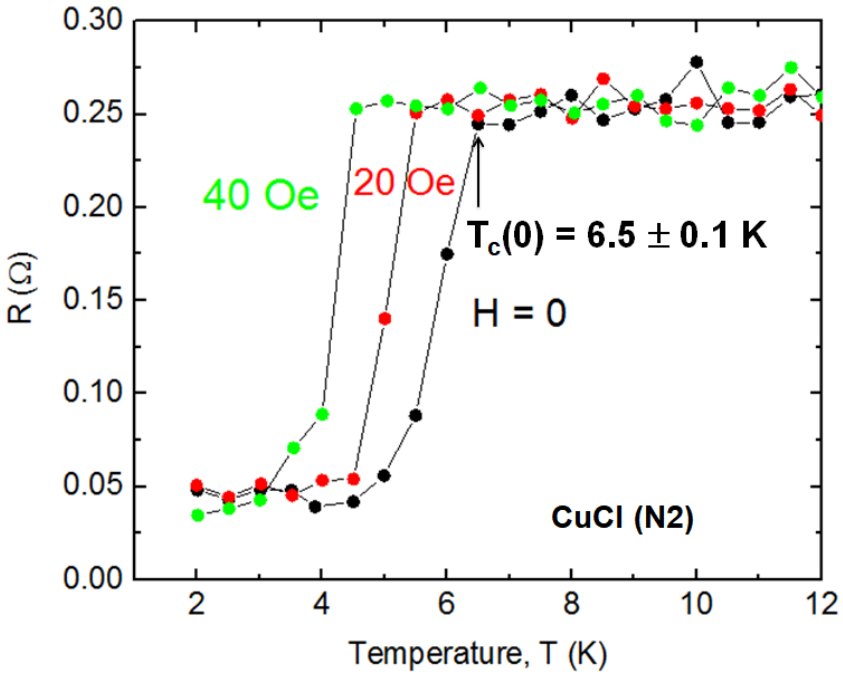

Fig.28. Resistance vs. temperature measured for low applied magnetic fieds. The characteristic for superconductors decreasing of the transition temperature with applied magnetic field is clear.

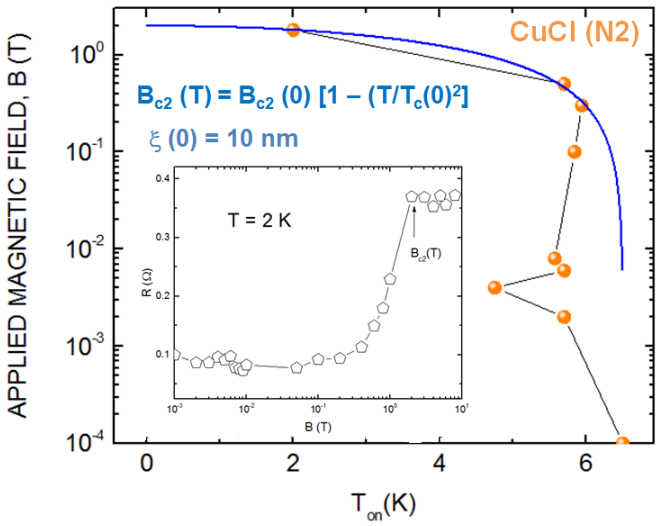

Fig. 29. Magnetic field (B) - temperature (T) phase diagram obtained for the sample CuCl(N2). The blue solid line corresponds to the equation $B_{c2}(T) = B_{c2}(0)[1-(T/T_c(0))^2]$ which gives the superconducting coherence length ξ(T = 0) = 10 nm. Inset shows magnetoresistance R(B) measured at T = 2 K demonstrating the superconductor-normal metal transition at the upper critical field $B_{c2}(T=2K) = 2$ T.

III. Main Conclusions.

Our results obtained under AFOSR support provided an unambigous experimental evidence for the CuCl oxidation at ambient conditions resulting in the formation of antiferromagnetic clinoatacamite $Cu_2Cl(OH)_3$ and CuO phases, intimately related to the measured localized superconductivity. Superconducting effects observed for $T < T_{N2} = 6.5$ K in the case of $Cu_2Cl(OH)_3$ and in the temperature interval $T_{N2} < T < 340$ K in the case of CuO coincide with fluctuating short-ranged ordered magnetization measured in these materials, resembling the behavior of RVB quantum spin liquid proposed for cuprates. Thus, our results strengthen the Anderson´s conjecture on superconductivity in CuCl and may have far-reaching consequences.

The obtained results were presented in various invited talks and Program Review Meetings (see below), and currently are in the preparation for publication in scientific journals.

Two most recent Meetings:

1) "Signatures of Interface Superconductivity in Oxidized CuCl"

AFOSR SUPERCONDUCTIVITY PROGRAM REVIEW

University of Houston Science Center – Room 102

April 26, 2018

2)" Insulator-Metal Transition and Superconductivity in CuCl"

2019 SOARD Program Review
March 19-20, 2019

Santiago, Chile